Critical metal enrichment in crustal melts: the role of metamorphic mica

Barbara E. Kunz*, Clare J. Warren, Frances E. Jenner, Nigel B.W. Harris, Tom W. Argles

School of Environment, Earth and Ecosystem Sciences, The Open University, Walton Hall, Milton Keynes, MK7 6AA, UK

*Corresponding author: barbara.kunz@open.ac.uk

Twitter: @KunzBE, @geologyclare, @tomargles

This manuscript is a non peer-reviewed preprint submitted to EarthArXiv in April 2022. It also has been submitted for publication in Geology. Subsequent versions of this manuscript may have revised content. Please feel free to contact any of the authors; we welcome feedback.

Critical metal enrichment in crustal melts: the role of metamorphic mica

Barbara E. Kunz*, Clare J. Warren, Frances E. Jenner, Nigel B.W. Harris, Tom W. Argles

School of Environment, Earth and Ecosystem Sciences, The Open University, Walton Hall, Milton Keynes, MK7 6AA, UK

Contact: barbara.kunz@open.ac.uk

ABSTRACT

Rare metals like Li, Be, V, Co, Nb, In, Cs, Sn, Ta, and W are considered critical resources and can be significantly enriched in granites and pegmatites. However the mechanisms of their enrichment in granitic magmas remain poorly understood. Many metal-enriched granitic magmas form through mica dehydration reactions during high-grade metamorphism. The preferential incorporation of these metals into micas provides a mechanism for their concentration and mobilisation during crustal anatexis. Comprehensive datasets of these elements and their partitioning in metamorphic micas across different metamorphic grades are currently lacking. We present the first extensive *in-situ* LA-ICP-MS element dataset collected from metasediment-hosted muscovite and biotite from three different metamorphic cross-sections traversing sub-greenschist (~400°C) to granulite-facies conditions (>900°C). Within the same sample Li, V, Co, Cs, and Ta are more concentrated in biotite, while Be, In, Sn, and W concentrations are higher in muscovite. Sub-solidus micas record only non-systematic compositional variations between samples. Supra-solidus biotites show systematic depletion in Li, Be, Sn and Cs and enrichment in V and Co with increasing temperature in the highest-grade (muscovite-absent) samples. Indium and W concentrations reach peak

concentrations in biotite at 750°C and 850°C respectively. Muscovites record systematic enrichment in In and W and depletion in Be, Sn and Cs with increasing metamorphic grade. These distinctive trends appear independent of geological/tectonic setting (i.e. continental collision and crustal thinning). Our dataset highlights the importance of higher-temperature melting (>750°C) and in particular, biotite breakdown reactions for the release of Li, Be, Sn, Cs and W into crustal melts.

INTRODUCTION

Most enriched granites and pegmatites are highly peraluminous, suggesting they formed via mica-melting reactions from metasedimentary protoliths (e.g., Patiño Douce and Harris, 1998; Cerny et al., 2012). During these reactions, trace elements that are hosted in micas may be released into the melt (Dahl et al., 1993). Along with enriched protolith compositions (Clemens et al., 2009; Romer and Kroner 2016; Wolf et al., 2018), melting reactions may play an important role in generating crustal magmas that are sufficiently enriched to eventually fuel formation of critical metal deposits at shallower levels in the crust (e.g., Linnen et al., 2012; London, 2018). Both fluid-present and fluid-absent reactions involving micas will generate melt, with muscovite melting at lower temperatures and biotite melting at higher temperatures (e.g., Weinberg and Hasalová, 2016).

The concentrations of different elements in these micas, and their behaviour during melting reactions, will influence the composition of the melt produced at different temperatures (Wolf et al., 2018). For example, melanosomes in migmatites that formed by muscovite-melting reactions at ~750°C in the Iberian Massif (Spain) are enriched in elements such as Li, Cs, Sn and W compared to the leucosomes. However both leucosomes and melanosomes in slightly higher temperature (800°C) migmatites generated by biotite-melting reactions recorded similar concentrations of these elements (Wolf et al., 2018). These data

63 suggested that higher temperature melting reactions release critical metals previously stored
64 in restitic mineral phases into the melt.

65 It is unclear if these trends and observations can be applied more generally to crustal
66 melting over a larger range of temperatures, different tectonic settings and different protolith
67 compositions. Additionally, direct comparisons between the compositions of leucosomes and
68 melanosomes are compromised by dilution, crystallisation, segregation or transport of the
69 magma that crystallises as the leucosome (Wolf et al., 2018). The role of sub- and supra-
70 solidus metamorphic reactions in concentrating and releasing critical elements is also poorly
71 constrained. These shortcomings make it difficult to assess why granites that are generated by
72 crustal melting have such variable critical element compositions. Here we present a new
73 approach for placing constraints on the partitioning of critical elements with increasing
74 temperatures during crustal melting. By measuring the concentrations of 57 elements *in-situ*
75 in muscovite and biotite from metapelites at different metamorphic grades, we have found
76 systematic changes in the concentrations of different critical metals as temperatures rise and
77 dehydration reactions initiate. This provides a new opportunity to constrain the input of
78 different critical metals into crustal melts at different stages of the metamorphic-melting
79 cycle.

80

81 **METHODS & SAMPLE MATERIAL**

82 We analysed trace element concentrations by LA-ICP-MS in muscovite and biotite in 22
83 samples from three different metamorphic cross-sections covering sub-greenschist to
84 granulite-facies conditions. Supplementary material S1–4 contains sample descriptions,
85 mineral assemblages, analytical methods and photomicrographs showing laser spot locations.
86 The full dataset of major and trace elements, secondary standards and all element plots are
87 presented in Table S5.

We selected samples from two different tectonic settings. The samples from the Himalayas were metamorphosed during continent-continent collision, whereas the samples from the Ivrea Zone received their metamorphic imprint during post-orogenic collapse and extension.

The eight samples labelled SK-10-XX were collected from a cross-section through the 5–10 km-thick Main Central Thrust in the Sikkim Himalaya, India. An inverted prograde metamorphic sequence is well-developed across this ductile structure, from low-greenschist (chlorite and biotite grades) at the lowest levels through to upper-amphibolite (kyanite and sillimanite grade) at the highest levels. The sampling localities, sample descriptions and pressure-temperature results are documented in detail in Mottram et al., (2014a,b). This sample set covers the onset of muscovite melting.

The four samples labelled N-XX were collected from the hanging wall of the Main Central Thrust in the Langtang Himalaya, Nepal, from higher structural levels and similar metamorphic grades to the highest-grade Sikkim samples. These samples were metamorphosed at kyanite to sillimanite grade, with coarser leucocratic streaks and patches interpreted as leucosome in samples N5 and N11, across the muscovite-out isograd.

The ten IZ-4XX samples were collected from the Val Strona di Omega, in the Ivrea Zone of the European Alps, Italy. They were metamorphosed at upper amphibolite to granulite facies conditions, and show both muscovite and biotite melting reactions. Sampling localities, sample descriptions and pressure-temperature results are documented in detail in Kunz et al. (2018) and Kunz and White (2019).

RESULTS

The within-sample average concentrations of 26 elements in biotite and muscovite shown in Fig. 1 are normalised to Bulk Silicate Earth concentrations (Palme and O'Neill,

2013) and plotted in order of increasing bulk partitioning behaviour (Jenner, 2017). Both biotite and muscovite record concentration variability within and between samples, and record enrichments and depletions in the concentrations of some critical elements (e.g., Sn, In, Cs) compared to the composition of the bulk continental crust. We have not observed any systematic patterns in element concentrations with petrographic location.

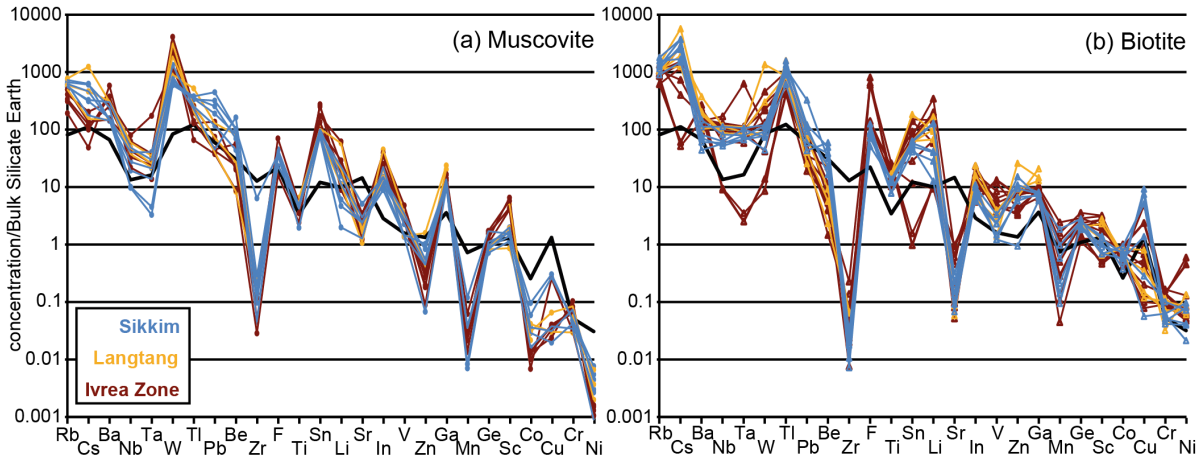

Fig. 1 Average trace element concentration per sample of (a) muscovite (b) biotite. Normalised to Bulk Silicate Earth (Palme and O'Neill, 2013); black line is the composition of the bulk continental crust (Rudnick and Gao, 2003); element ordering is based on bulk partitioning during differentiation of mid-ocean ridge basalts (Jenner, 2017).

Elemental concentrations in biotite vary more systematically than in muscovite particularly in the high-temperature samples from the Ivrea Zone compared to the samples from the lower grade Sikkim section (Figs. 2 and 3; Tab. S1). Specifically, there are systematic changes in the concentrations of Li, Be, V, Co, Nb, In, Sn, Cs, Ta, and W with increasing metamorphic grade that are all greater than analytical uncertainty; we have therefore focussed attention on these eleven elements. Additionally, there are clear differences in concentration between the different field areas that are most likely related to different bulk rock abundances of these elements.

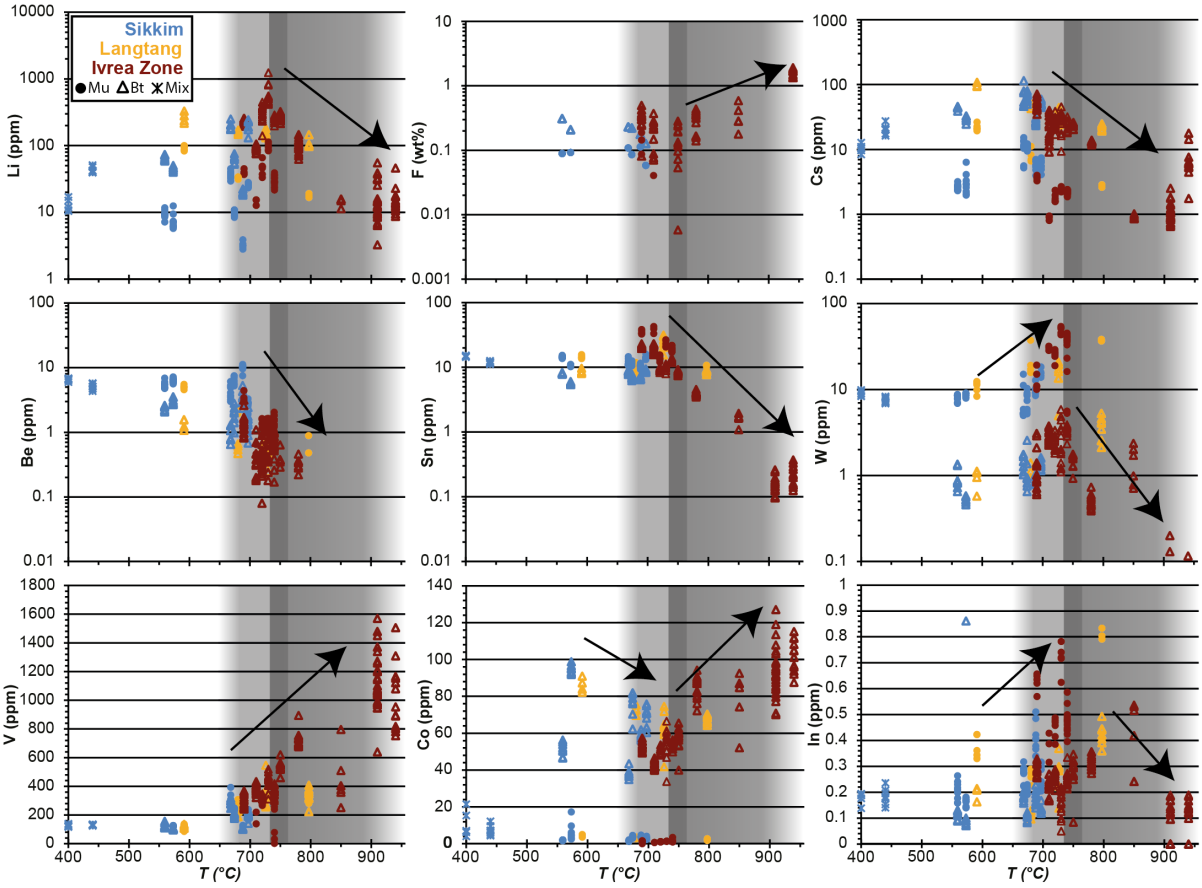

133

134 **Fig. 2** Concentrations of Li, F, Cs, Be, Sn, W, V, Co and In *vs.* peak metamorphic temperature. Grey
135 shaded areas represent muscovite- (light grey) and biotite-melting (dark grey) ranges.
136

137 Typically, biotite contains higher concentrations of Li, V, Co, Nb, Cs and Ta than
138 muscovite, whereas muscovite systematically hosts higher concentrations of Be, In, Sn and
139 W (Figs. 2 & 3). Concentrations of most elements in muscovite show little to no systematic
140 change with increasing metamorphic temperature, however In and W show increases at
141 supra-solidus temperatures and Li, Be and Cs show decreases but only in the Langtang
142 samples.

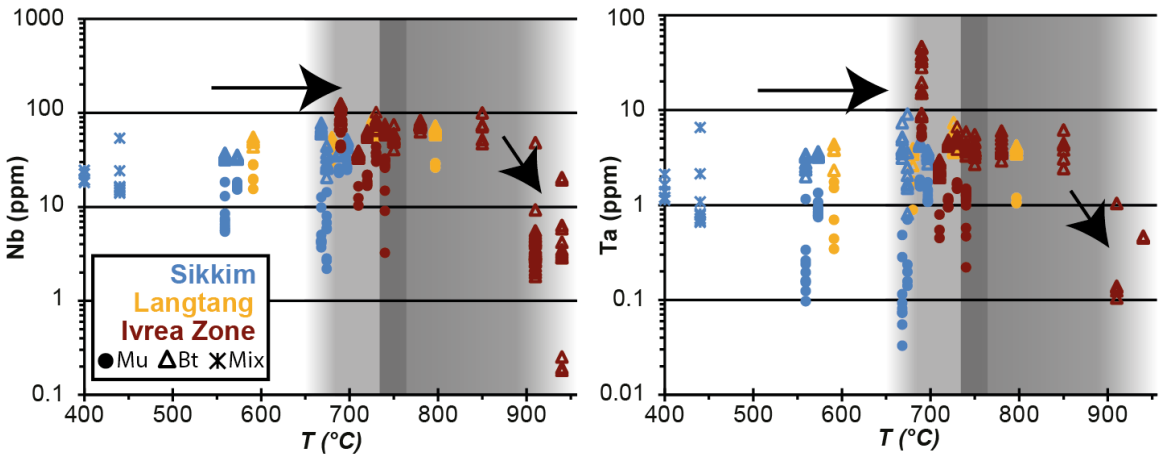

Fig. 3 Concentration of Nb and Ta *vs.* peak metamorphic temperature. Grey shaded areas represent muscovite- (light grey) and biotite-melting (dark grey) ranges.

Sub-solidus biotites in the Sikkim samples show no systematic changes in trace element concentration. Above solidus temperatures, biotite in the Langtang and Ivrea Zone samples show a gradual decrease in Li, Cs, Be and Sn concentrations and an increase in V and Co concentrations with increasing temperature (Fig. 2). Concentrations of In and W increase in biotite as temperatures increase to ~850 and 750°C respectively, after which concentrations decrease with increasing metamorphic grade (Fig. 2). Ta and Nb concentrations remain fairly constant in biotite with increasing metamorphic temperature, except in the two highest-grade samples that have abundant rutile (Fig. 3).

DISCUSSION

Critical metal concentrations in micas from metasediments from three different regions characterised by systematic changes in metamorphic grade show a systematic evolution with increasing metamorphic temperatures. While there is some variability within and across the different samples, most likely due to disequilibrium at low-grade metamorphic conditions or protolith heterogeneities, there are systematic overall trends in changes in concentration with temperature (Figs. 2).

Samples SK12 and SK15 are at the low-temperatures end of the series. Muscovite and biotite are commonly fine-grained, intergrown and appear in close association with chlorite. It is analytically challenging to acquire "clean" analyses. We therefore interpret the scatter in these analyses as due to mixing and chemical disequilibrium between the micas in the samples. Samples SK16–17 and N13, and samples SK19–22, N2 and IZ410 equilibrated at similar temperatures within uncertainty (550–600°C and 650–700°C respectively). In the subsolidus samples, the concentrations of most critical metals measured in the different mica types show little scatter, although there are significant differences in the concentrations of Li, Cs and Ta in both micas within and between samples. In the samples from Sikkim we observe a difference in Li and Ta concentrations in both micas across samples SK19–SK22 that all equilibrated at similar metamorphic temperatures. We interpret this as either: (i) reflecting differences in bulk composition and therefore different initial trace element abundance (e.g., Romer and Kroner, 2016), or (ii) reflecting differences in the continuity of this metamorphic sequence due to ductile deformation.

Importantly, our data show that Li, Cs and Ta (commonly hosted together in LCT-pegmatites) are predominantly hosted in biotite, while Be, Sn and W are predominantly hosted in muscovite (c.f. Dutrow et al., 1986; Dahl et al., 1993; Bea et al., 1994; Yang and Rivers, 2000; Neiva et al., 2002; Van Lichtervelde et al., 2008; Simons et al., 2017). The partitioning between biotite and muscovite can be explained by differences in site and interlayer site preferences of these elements (Dahl et al., 1993). The apparent increase in concentration of V, Co and In in biotite with increasing metamorphic grade could be an effect of decreasing modal abundance of biotite. However, the concentration increase starts at the onset of muscovite melting when the modal abundance of biotite is still increasing. Therefore we interpret the observed trends for these elements as resulting from differential partitioning in the presence of a melt phase. However the increase of W in muscovite does coincides with

188 the decrease in modal abundance of muscovite, suggesting that this might be a modal
189 abundance effect.
190
191 **Implications for the formation of enriched granites and pegmatites**
192 Our dataset demonstrates the importance of melting reactions involving biotite for the
193 concentration (in the restite) and release (into the melt) of a number of critical metals,
194 specifically Li, Be, Sn, Cs and W. Biotite is widely present in a variety of bulk-rock
195 compositions and is a known host of critical metals (e.g. Dahl et al., 1993; Evensen and
196 London, 2002). Our data show that concentrations of these elements in metapelitic biotite
197 remains approximately constant until the onset of biotite dehydration melting reactions, when
198 these elements are released into the melt. Our findings are in agreement with bulk rock data
199 from the Ivrea Zone (Bea and Montero, 1999) that show a similar depletion in bulk rock for
200 Li, Be Cs and an increase in V with metamorphic grade.
201 This scenario of high-temperature biotite melting as the key for the enrichment of Li-
202 Cs-Ta in the melt is in conflict with previous hypothesis of LCT-enriched pegmatites being
203 generated by minimum-temperature melting of muscovite (e.g. Cerny 1991; Romer and
204 Kroner, 2015, 2016). Instead, our data suggest that enrichment of LCT-enriched granitic
205 magmas most likely occurs during low-volume biotite melting of a mostly muscovite-absent
206 assemblage, a scenario that has also been argued for granitic Sn enrichment (Wolf et al.
207 2018) and the enrichment patterns of successive granite suites of the Cornubian Batholith in
208 Cornwall, UK (Simons et al., 2016).
209 Biotite provides the source of these elements as well as a mechanism for allowing
210 more effective melt and metal transport. Crustal melts are viscous (Rutter and Neumann,
211 1995) and therefore difficult to mobilise without additional help, e.g. from pervasive ductile
212 deformation or the addition of fluxing elements such as F, which lower melt viscosity

(Dingwell et al., 1996). Additionally, F allows metals to be transported in the melt more readily through complexing (London, 1987). High-temperature biotite can host F at weight-% levels (Finch and Tomkins, 2016); in our samples the Sikkim and the Ivrea Zone biotites contain higher F concentrations than muscovite (0.13–1.6 wt% F compared to 0.04–0.16 wt% F respectively; Fig 2).

Sn and W enrichments in granites have been linked to high-temperature melting of a biotite-rich source (Romer and Kroner, 2016; Wolf et al., 2018). Our data show that, in general, concentrations of Sn and W are higher in muscovite than in co-hosted biotite. Concentrations of W in muscovite increase slightly with metamorphic grade; we do not observe systematic changes of Sn concentrations in muscovite with metamorphic grade. In contrast, biotite from the Ivrea Zone and Langtang samples show clear decreases in Sn and W concentrations with increasing metamorphic grade. This observation supports the theory of higher-temperature melting being critical for melt enrichment (Wolf et al., 2018; Michaud et al., 2021). However we do not observe sequestering of Sn into biotite across the muscovite-melting temperature interval, as previously suggested (Wolf et al 2018).

Further investigation into different biotite melting reactions, including those which are fluid-absent or fluid-present, are needed to understand the conditions/reactions under which critical metal release is optimised and therefore provides the highest potential for melt enrichment. Biotite is also a key constituent in non-pelitic metasesediments (e.g. meta-graywackes) that may also be source rocks for enriched granites and pegmatites. Focus on biotite-melting reactions across a range of metasedimentary bulk compositions is therefore key to constraining how and under which conditions critical metal enriched granites and pegmatites form.

CONCLUSIONS

Micas are the main reactant during the dehydration melting of metasediments. As micas host significant concentrations of many critical metals, their breakdown facilitates the transfer of these metals from metamorphosed country rocks into melts. Our data show that prograde sub-solidus metamorphic reactions do not lead to systematic changes in the concentrations of different critical metals in micas. Upon crossing the muscovite dehydration solidus both muscovite and biotite concentration for Cs and Be start to decrease, while W concentration increase. Once conditions for biotite dehydration melting are reached, concentrations of Li, Be, Sn, Cs, & W in biotite decrease markedly as they are released into the melt.

ACKNOWLEDGMENTS

We'd like to thank Giulia Degli-Alessandrini for help with EMPA work at the OU. Kathryn Goodenough and Richard Shaw (British Geological Survey) for fruitful discussions and Catherine Mottram for sending us her thin sections from the Sikkim section. BEK and FEJ acknowledge funding from Natural Environment Research Council (NERC) grant NE/P017045/1 (From Arc Magmas to Ore Systems).

REFERENCES CITED

Bea, F., and Montero, P., 1999, Behavior of accessory phases and redistribution of Zr , REE , Y , Th , and U during metamorphism and partial melting of metapelites in the lower crust : An example from the Kinzigite Formation of Ivrea-Verbano , NW Italy: Geochimica et Cosmochimica Acta, v. 63, p. 1133–1153.

Bea, F., Pereira, M.D., and Stroh, A., 1994, Mineral/leucosome trace-element partitioning in a peraluminous migmatite (a laser ablation-ICP-MS study): Chemical Geology, v. 117, p. 291–312, doi:10.1016/0009-2541(94)90133-3.

Černý, P., 1991, Fertile granites of Precambrian rare-element pegmatite fields: is geochemistry controlled by tectonic setting or source lithologies? Precambrian Research, v. 51, p. 429–468, doi:10.1016/0301-9268(91)90111-M.

Cerny, P., London, D., and Novak, M., 2012, Granitic Pegmatites as Reflections of Their Sources: Elements, v. 8, p. 289–294, doi:10.2113/gselements.8.4.289.

Clemens, J.D., Helps, P.A., and Stevens, G., 2009, Chemical structure in granitic magmas - A signal from the source?, *in* Earth and Environmental Science Transactions of the Royal Society of Edinburgh, Royal Society of Edinburgh Scotland Foundation, v. 100, p. 159–172, doi:10.1017/S1755691009016053.

Dahl, P.S., Wehn, D.C., and Feldmann, S.G., 1993, The systematics of trace-element partitioning between coexisting muscovite and biotite in metamorphic rocks from the Black Hills, South Dakota, USA: Geochimica et Cosmochimica Acta, v. 57, p. 2487–2505.

Dingwell, D.B., Romano, · C, and Hess, K.-U., 1996, The effect of water on the viscosity of a haplogranitic melt under P-T-X conditions relevant to silicic volcanism: Contrib Mineral Petrol, v. 124, p. 19–28.

Dutrow, B.L., Holdaway, M.J., and Hinton, R.W., 1986, Lithium in staurolite and its petrologic significance: Contributions to Mineralogy and Petrology 1986 94:4, v. 94, p. 496–506, doi:10.1007/BF00376341.

Evensen, J.M., and London, D., 2002, Experimental silicate mineral/melt partition coefficients for beryllium and the crustal Be cycle from migmatite to pegmatite: Geochimica et Cosmochimica Acta, v. 66, p. 2239–2265, doi:10.1016/S0016-7037(02)00889-X.

Finch, E.G., and Tomkins, A.G., 2017, Fluorine and chlorine behaviour during progressive dehydration melting: Consequences for granite geochemistry and metallogeny: Journal of Metamorphic Geology, v. 35, p. 739–757, doi:10.1111/jmg.12253.

Jenner, F.E., 2017, Cumulate causes for the low contents of sulfide-loving elements in the continental crust: Nature Geoscience 2017 10:7, v. 10, p. 524–529, doi:10.1038/ngeo2965.

Kunz, B.E., Regis, D., and Engi, M., 2018, Zircon ages in granulite facies rocks: decoupling from geochemistry above 850 °C? Contributions to Mineralogy and Petrology 2018 173:3, v. 173, p. 1–21, doi:10.1007/S00410-018-1454-5.

Kunz, B.E., and White, R.W., 2019, Phase equilibrium modelling of the amphibolite to granulite facies transition in metabasic rocks (Ivrea Zone, NW Italy): Journal of Metamorphic Geology, v. 37, p. 935–950, doi:10.1111/JMG.12478.

Lichtervelde, M., Grégoire, M., Linnen, R.L., Béziat, D., and Salvi, S., 2008, Trace element geochemistry by laser ablation ICP-MS of micas associated with Ta mineralization in the Tanco pegmatite, Manitoba, Canada: Contributions to Mineralogy and Petrology, v. 155, p. 791–806, doi:10.1007/s00410-007-0271-z.

Linnen, R.L., Van Lichtervelde, M., and Cerny, P., 2012, Granitic Pegmatites as Sources of Strategic Metals: Elements, v. 8, p. 275–280, doi:10.2113/gselements.8.4.275.

London, D., 1987, Internal differentiation of rare-element pegmatites: Effects of boron, phosphorus, and fluorine: Geochimica et Cosmochimica Acta, v. 51, p. 403–420, doi:10.1016/0016-7037(87)90058-5.

306 London, D., 2018, Ore-forming processes within granitic pegmatites: Ore Geology Reviews,
307 v. 101, p. 349–383, doi:10.1016/j.oregeorev.2018.04.020.

308 Michaud, J.A.-S., Pichavant, M., and Villaros, A., 2021, Rare elements enrichment in crustal
309 peraluminous magmas: insights from partial melting experiments: Contributions to
310 Mineralogy and Petrology, v. 176, p. 96, doi:10.1007/s00410-021-01855-9.

311 Mottram, C.M., Argles, T.W., Harris, N.B.W., Parrish, R.R., Horstwood, M.S.A., Warren,
312 C.J., and Gupta, S., 2014, Tectonic interleaving along the Main Central Thrust, Sikkim
313 Himalaya: Journal of the Geological Society, v. 171, p. 255–268, doi:10.1144/JGS2013-
314 064.

315 Mottram, C.M., Warren, C.J., Regis, D., Roberts, N.M.W., Harris, N.B.W., Argles, T.W., and
316 Parrish, R.R., 2014, Developing an inverted Barrovian sequence; insights from monazite
317 petrochronology: Earth and Planetary Science Letters, v. 403, p. 418–431,
318 doi:10.1016/J.EPSL.2014.07.006.

319 Neiva, A.M.R., Silva, M.M.V.G., Gomes, M.E.P., and Campos, T.F.C., 2002, Geochemistry
320 of coexisting biotite and muscovite of Portuguese peraluminous granitic differentiation
321 series: Chemie der Erde, v. 62, p. 197–215, doi:10.1078/0009-2819-00007.

322 Palme, H., and O'Neill, H., 2013, Cosmochemical Estimates of Mantle Composition, *in*
323 Treatise on Geochemistry: Second Edition, v. 3, p. 1–39, doi:10.1016/B978-0-08-
324 095975-7.00201-1.

325 Patiño Douce, A.E., and Harris, N., 1998, Experimental constraints on Himalayan anatexis:
326 Journal of Petrology, v. 39, p. 689–710, doi:10.1093/petroj/39.4.689.

327 Romer, R.L., and Kroner, U., 2015, Sediment and weathering control on the distribution of
328 Paleozoic magmatic tin–tungsten mineralization: Mineralium Deposita, v. 50, p. 327–
329 338, doi:10.1007/s00126-014-0540-5.

330 Rutter, E.H., and Neumann, D.H.K., 1995, Experimental deformation of partially molten
331 Westerly granite under fluid-absent conditions, with implications for the extraction of
332 granitic magmas: Journal of Geophysical Research: Solid Earth, v. 100, p. 15697–
333 15715, doi:10.1029/94JB03388.

334 Simons, B., Andersen, J.C.Ø., Shail, R.K., and Jenner, F.E., 2017, Fractionation of Li, Be,
335 Ga, Nb, Ta, In, Sn, Sb, W and Bi in the peraluminousEarly Permian Variscan granites of
336 the Cornubian Batholith: Precursorprocesses to magmatic-hydrothermal mineralisation:
337 Lithos, v. 278–281, p. 491–512, doi:10.1016/j.lithos.2017.02.007.

338 Simons, B., Shail, R.K., and Andersen, J.C.O., 2016, The petrogenesis of the Early Permian
339 Variscan granites of the Cornubian Batholith: Lower plate post-collisional peraluminous
340 magmatism in the Rhenohercynian Zone of SW England: Lithos, v. 260, p. 76–94,
341 doi:10.1016/j.lithos.2016.05.010.

342 Tischendorf, G., Förster, H.-J., and Gottesmann, B., 2001, Minor- and trace-element
343 composition of trioctahedral micas: a review: Mineralogical Magazine, v. 65, p. 249–
344 276, doi:10.1180/002646101550244.

Weinberg, R.F., and Hasalová, P., 2015, Water-fluxed melting of the continental crust: A review: Lithos, v. 212–215, p. 158–188, doi:10.1016/j.lithos.2014.08.021.

Wolf, M., Romer, R.L., Franz, L., and López-Moro, F.J., 2018, Tin in granitic melts: The role of melting temperature and protolith composition: Lithos, v. 310–311, p. 20–30, doi:10.1016/j.lithos.2018.04.004.

Yang, P., and Rivers, T., 2000, Trace element partitioning between coexisting biotite and muscovite from metamorphic rocks, Western Labrador: Structural, compositional and thermal controls: Geochimica et Cosmochimica Acta, v. 64, p. 1451–1472, doi:10.1016/S0016-7037(99)00425-1.

SUPPLEMANTARY MATERIAL

APPENDIX 1. Sample description

APPENDIX 2. Table with mineral assemblages

APPENDIX 3. Detailed method description for LA-ICP-MS analysis

APPENDIX 4. LA-ICP-MS spot location

APPENDIX 5. Major and trace element data table for samples and secondary standards